

The Nature of Gold Mineralization in the Archean Sunrise Dam Gold Deposit in Western Australia

Yoo-Hyun Sung^{1*} and Sang-Hoon Choi²

¹Research & Development Team, Technical Institute, Korea Resources Corporation

²Department of Earth and Environmental Sciences, Chungbuk National University, Cheongju 361-763, Korea

호주 Sunrise Dam 광상의 금 광화작용

성유현^{1*} · 최상훈²

¹한국광물자원공사 기술연구소, ²충북대학교 지구환경과학과

호주 Yilgarn Craton의 동부 Laverton Tectonic Zone에 위치하는 Sunrise Dam 금광은 서호주에서 지난 10년간 두번째로 가장 많은 금을 생산한 광산이다. 광상 주변의 지질은 화산암류와 이들의 상부에 산출하는 저탁 퇴적암류 그리고 이들을 관입하여 산출하는 시생대 및 원생대 석영섬록암 및 암맥류 등으로 구성된다. 이들 암석들은 북북동 방향의 비대칭 Spartan 배사를 이루고 있으며, 광상은 본 배사의 서쪽 날개부에 발달된 북동-남서 방향의 전단대를 따라 배태된 20여개의 광체로 구성되어 있다. 본 광상은 광물조합 등에 의하여 확실하게 구분되는 5개의 열수광화시기 (D₁, D₂, D₃, D_{4a}, D_{4b})로 구분된다. 이들 열수광화시기 중 금 광화작용이 가장 우세하게 진행된 시기는 D_{4a} 열수광화기이며, D_{4b} 열수광화기에 그 다음으로 우세한 금 광화작용이 야기되었다. 이들 열수광화시기의 금 광화작용은 주로 황철석 및 사면동석의 침전과 밀접하게 관련되어 있다.

주요어 : Sunrise Dam 금광상, Yilgarn Craton, 호주서부

The Sunrise Dam gold deposit is located approximately 850 km ENE of Perth, in the eastern part of the Yilgarn Craton, Western Australia. The mine has produced approximately 153 t of Au at an average grade of 4.2 g/t, which stands for the most significant gold discoveries during the last decade in Western Australia. The deposit occurs in the Laverton Tectonic Zone corresponding to the corridor of structural complexity in the Laverton greenstone belt, and characterized by tight folding and thrusting. The mine stratigraphy consists of a complexly deformed and altered volcanoclastic and volcanic rocks. These have been overlain by a turbidite sequence containing generally well-sorted siltstones, sandstones and magnetite-rich shales, which are consistently fining upwards. These sequences have been intruded by quartz diorite, ultramafic dikes, and rhyodacite porphyry (Archean), and lamprophyre dikes (Palaeoproterozoic). These rocks constitute the asymmetric NNE-trending Spartan anticline with north-plunging thrust duplication of the BIF unit. The deposit is located on the western limb of this structure. Transported, fluvial-lacustrine and aeolian sediments lie unconformably over the deposit showing significant variation in relief. Gold mineralization occurs intermittently along a NE-trending corridor of ca. 4.5 km length. The 20 currently defined orebodies are centered on a series of parallel, gently-dipping (~30°) and NE-SW trending shear zones with a thrust-duplex architecture and high-strain characteristics. The paragenetic sequence of the Sunrise Dam deposit can be divided into five hydrothermal stages (D₁, D₂, D₃, D_{4a}, D_{4b}), which are supported by distinctive features of the mineralogical assemblages. Among them, the D_{4a} stage is the dominant episode of Au deposition, followed by the D_{4b} stage, which is characterized by more diverse ore mineralogy including base metal sulfides, sulfosalts, and telluride minerals. The D_{4a} stage contains higher proportions of microscopic free gold (48%) than D_{4b} stage (12%), and pyrite is the principal host for native gold (electrum) followed by tetrahedrite-group minerals in both stages.

Key words : Sunrise Dam gold deposit, Yilgarn Craton, Western Australia

*Corresponding author: yhsung@kores.or.kr

1. Introduction

The Sunrise Dam gold deposit is located approximately 850 km ENE of Perth, in the eastern part of the Yilgarn Craton, Western Australia (Fig. 1). The mine is owned and operated by Anglo-Gold Ashanti Australia Ltd. and has produced approximately 153 t of Au at an average grade of 4.2 g/t (Nugus and Biggam, 2007), which stands for the most significant gold discoveries during the last decade in Western Australia.

The deposit contains a structurally complex series of gold-rich ore bodies with a variety of deformation fabrics that influence the nature, geometry and distribution of the mineralization (Nugus and Biggam, 2007). Therefore, considerable efforts have been devoted to the determination of lithology, ore fluid characteristics, and the structural controls on the gold mineralization at Sunrise Dam (e.g., Brown *et al.*, 2002a; Brown *et al.*, 2002b; Brown *et al.*, 2003; Cassidy and Hagemann, 2001; Nugus *et al.*, 2005a; Nugus *et al.*, 2005b; Nugus *et al.*, 2005c; Nugus *et al.*, 2006). However, mineral paragenesis, the nature of gold mineralogy and its

(re-)distribution in accord with the multiple deformation events are remained unclear, although mineralogical data is crucial not only to optimize gold recoveries, but also to establish a genetic model for the Archean orogenic gold system.

The deposit contains both free-milling and refractory Au ores, and the average Au recovery is about 80%. The refractory Au ores at Sunrise Dam consist mainly of arsenian pyrite and arsenopyrite (Sung *et al.*, 2009). The aim of the paper is thus to characterize the ore minerals, their associations, distribution, and paragenetic sequence in the Sunrise Dam deposit, and use this information provide mineralogical basis of ore processing as well as an insight into the various mechanisms of Au enrichment in a world-class orogenic Au deposit.

2. Geological Setting

2.1. Regional Geology

The Eastern Goldfields Province (EGP) is an intensely mineralized Late Archean granite-greenstone terrane, which is approximately 900 km long and 400 km wide, occupying the eastern third of

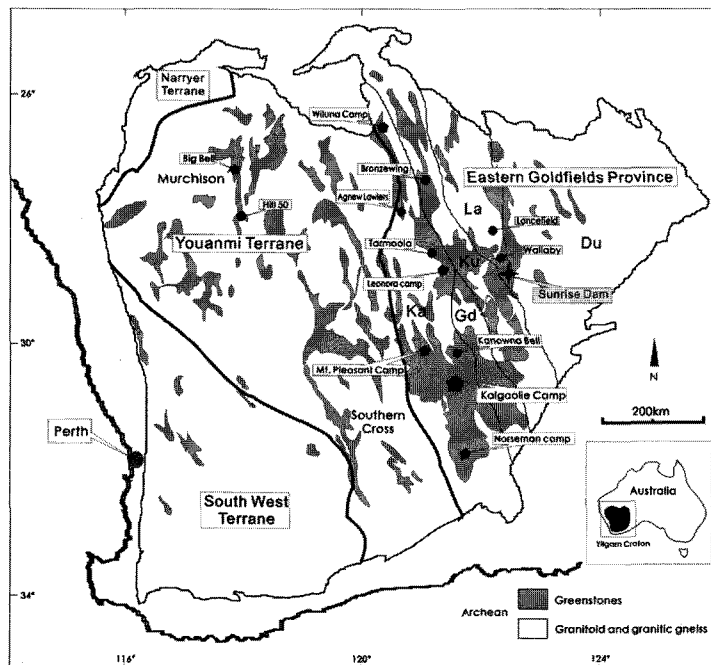


Fig. 1. Geological map of Yilgarn Craton of Western Australia showing terrane boundaries and gold deposit locations (modified after Cassidy *et al.* 2006). Abbreviations: Ka: Kalgoorlie terrane; Gd: Gindalbie terrane; Ku: Kurnalpi terrane; La: Laverton terrane; Du: Duketon-Burtville terrane.

the Yilgarn Craton (Myers, 1997; Griffin, 1990)(Fig. 1). It is characterized by many major NW-NNW trending faults, large areas of granitoids, and generally narrow, linear to arcuate greenstone belts which are more abundant than any other provinces in the craton (Griffin, 1990).

Tectonically, the EGP consists of five tectono-stratigraphic terranes defined by their distinct volcanic facies, geochemistry, and age of volcanism (Myers and Hickman, 1990; Swager, 1997). From southwest to northeast, these are the Kalgoorlie, Gindalbie, Kurnalpi, Laverton, and Duketon-Burtville Terranes (Fig. 1). Each terrane is divided into structurally bound domains that preserve dismembered, thrust-repeated parts of the succession and locally have distinct volcanic facies relationships (Barley *et al.*, 2002; Swager, 1997; Cassidy *et al.*, 2006). The Kalgoorlie and Gindalbie Terranes are characterized by tonalite-trondhjemite-dacite (TTD) volcanism and interpreted as transtensional, deep-marine intra-arc basins accompanied by westward-dipping subduction zone (Cassidy *et al.*, 2006; Krapez *et al.*, 2000; Barley *et al.*, 1989). The Kurnalpi Terrane is typified by calc-alkaline volcanic rocks which were formed within arc-related terranes along the same convergent margin (Barley *et al.*, 2002). The Laverton Terrane sequence may represent autochthonous basement including mafic to ultramafic volcanic rocks, BIF, and fine grained volcanogenic sedimentary rocks (Cassidy *et al.*, 2006). The Duketon-Burtville Terrane consists of three poorly defined domains containing metamorphosed mafic and felsic volcanic and sedimentary sequences of undetermined age (Cassidy *et al.*, 2006). The Sunrise Dam gold deposit is located in Laverton Tectonic Zone (Hallberg, 1985) within the Laverton Greenstone Belt (LGB) of the Laverton Terrane (Fig. 1). In recent years, the LGB has become a major center of gold production, hosting two world-class (>100 t Au) gold deposits (e.g., Sunrise Dam and Wallaby) with a total contained gold endowment of over 700 t (Salier *et al.*, 2005).

2.2. Geology of the Sunrise Dam Deposit

The Sunrise Dam gold deposit is located in the Laverton Tectonic Zone corresponding to the corridor of structural complexity in the LGB, and characterized by tight folding and thrusting (New-

ton *et al.*, 1998). The Cleo Upper Shear (CUS) and the Sunrise Shear Zone (SSZ) are major structural features associated with the deposit (Fig. 2). The CUS occurs in the hanging wall of the SSZ and is truncated by erosion in the western portion of the Sunrise pit. There are numerous subsidiary splay shears that branch upwards from the hanging wall of the SSZ (e.g., Margies, Placer upper, and Ulu flat Shear). Western Shear Zone (WSZ) and Watu Fault Zone (WFZ) are steeply dipping, low strain shear zones that are recognized between the CUS and the SSZ (Fig. 2).

The mine stratigraphy consists of a complexly deformed and altered package of shallowly NW-dipping units dominated by volcanoclastic and volcanic rocks of intermediate affinity (Nugus and Biggam, 2007). These have been overlain by a turbidite sequence containing generally well-sorted siltstones, sandstones and magnetite-rich shales (BIF, *sensu lato*), which are consistently fining upwards. The compositions of silts and sands are similar to that of the underlying intermediate volcanic packages (Nugus and Biggam, 2007). These sequences have been intruded by quartz diorite, ultramafic dikes, and rhyodacite porphyry which are constrained to be of Archean age (Ojala *et al.*,

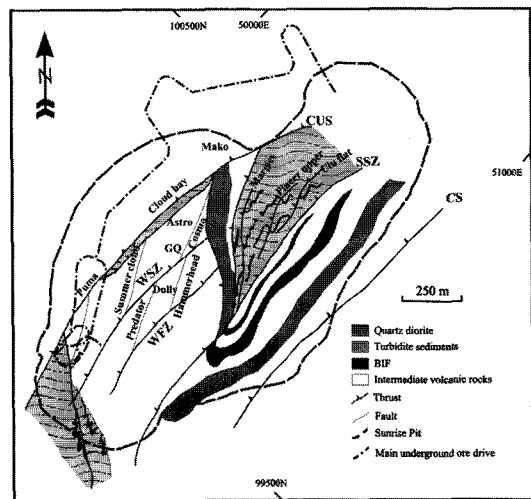


Fig. 2. Simplified geological plan view of the Sunrise Dam open pit showing major lithologies, structures, and ore bodies (modified after Nugus and Biggam 2007). Abbreviations: CUS=Cleo Upper Shear; SSZ=Sunrise Shear Zone; CS=Carey Shear; WSZ=Western Shear Zone; WFZ=Watu Fault Zone. Mine grid is rotated 45°E of true north.

1993), and lamprophyre dikes of Palaeoproterozoic age (Brown *et al.*, 2002a). These rocks constitute the asymmetric NNE-trending Spartan anticline with north-plunging thrust duplication of the BIF unit (Newton *et al.*, 2002). The deposit is located on the western limb of this structure. Transported, fluvial-lacustrine and aeolean sediments lie unconformably over the deposit showing significant variation in relief.

3. Gold Mineralization

3.1. Structural Control and Mineralizing Events

Gold mineralization occurs intermittently along a NE-trending corridor of ca. 4.5 km length, characterized by the presence of strongly magnetic BIF sequences (Newton *et al.*, 2002). The 20 currently defined orebodies are centered on a series of parallel, gently-dipping ($\sim 30^\circ$) and NE-SW trending shear zones with a thrust-duplex architecture and high-strain characteristics: e.g., Cleo Upper Shear (CUS), Sunrise Shear Zone (SSZ), and Carey Shear (CS) (Fig. 2). Such gently-dipping structures, characteristic of many orogenic gold deposits in the LGB (e.g. Wallaby, Granny Smith, Lancefield, Jubilee etc.), usually carry a significant proportion of the ore. A number of orebodies in the deposit are also found within steep, low-strain shear zones that develop between the gently dipping shear zones, namely Western Shear Zone (WSZ) and Watu Fault Zone (WFZ). The WSZ dips $40\text{--}70^\circ$ to the NW and has an overall sigmoidal shape, while the WFZ has a sub-vertical dip and strikes $N30^\circ E$ at the southern end and $N65^\circ E$ at the northern end. These lodes carry higher and more consistent grades than the SSZ-hosted.

N-E striking structures contain $\sim 79\%$ of the Au. The remaining portion (21%) is hosted by N-S (010°) striking structures; e.g. the Summer Cloud, Predator, Hammer Head, and Cosmo ore bodies (Fig. 2), which comprise an important proportion of the current underground resources. These NS-trending orebodies were controlled by steeply-dipping faults which developed as backthrusts to the SSZ (Nugus *et al.*, 2005c).

The inherent complexity in the deformation history results from the focusing of deformational fabrics within discrete zones where overprinting

and reactivation have occurred in several stages (Nugus and Biggam, 2007). This and extensive hydrofracturing during later deformation stages are extremely important controls on the extent and tenor of mineralization within the deposit. Mineralogical studies have established a paragenetic sequence consisting of five hydrothermal stages (D_1 , D_2 , D_3 , D_{4a} and D_{4b}) which are generally in accord with the major deformation events at Sunrise Dam gold deposit. The structural characteristics and the nature of the mineralization are summarized in Table 1.

The earliest deformation event (D_1) formed F_1 folds and thrusts (i.e., SSZ, CUS and CS) in response to N-S compression and shortening (S_1) (Nugus *et al.*, 2005b). The second event (D_2) was characterized by regional E-W shortening associated with the formation of the Spartan Anticline (F_2 fold) and penetrative N-S trending cleavage (S_2). These events were associated with carbonate-chlorite-sericite hydrothermal alteration but minor Au mineralization occurred only in the D_1 stage. However, the extent and role of these hydrothermal events is difficult to estimate in the mine area due to strong overprinting by the D_3 and D_4 events.

The third deformation event (D_3) led to the formation of WSZ and WFZ during NNW-SSE to NW-SE oriented stress (Nugus and Biggam 2007). This was also responsible for reactivation of S_1 and S_2 with sinistral strike-slip movement as well as development of S_3 fractures and NE-trending extensional vein arrays with high grade of Au mineralization. However, within the SSZ, gold mineralization in discrete D_3 shear zones is generally medium grade, but locally As-rich veins tend to have high grades (Nugus *et al.*, 2005a).

The last deformation event (D_4) resulted from NW-SE shortening with local dextral reactivation on S_3 surfaces containing extensional auriferous veins (Nugus and Biggam, 2007). The D_4 veins can be subdivided into steeper-dipping, early (D_{4a}) and gentle-dipping, late veins (D_{4b}) with different mineralogy, texture and geochemical signatures. The D_{4a} veins host significant amounts of coarse gold mineralization and have a strike continuity that extends for more than 1 km with narrow alteration haloes between 0.5–5 m laterally. The D_{4b} veins are closely associated with distinct fault zones that are shallow west dipping with similar

Table 1. Comparison of deformation events proposed for the LGB and the Sunrise Dam deposit

Event	LGB	Sunrise Dam
	Ojala (1995); Blewett <i>et al.</i> (2002)	Nugus <i>et al.</i> (2005b); Nugus and Biggam (2007)
D _E	NNW-SSE extension <ul style="list-style-type: none"> ● low angle E-W to NE-SW trending shear zones ● komatiite intrusion (ca. 2705 Ma) ● basin development 	-
D ₁	N-S to NW-SE compression <ul style="list-style-type: none"> ● NE-SW trending thrust faults ● reactivation of D_E faults ● stratigraphic repetition ● isoclinal and recumbent folding 	N-S shortening <ul style="list-style-type: none"> ● F₁ fold and thrust: NNW→SSE transport (SSZ, CUS) ● shearing zones with sub horizontal L₁, S₁ ● shear parallel veins (0.25–1.5 g/t Au)
D ₂	ENE-WSW to E-W compression <ul style="list-style-type: none"> ● reactivation of D₁ structures→upright fold ● extensive imbricate N-S thrust faults ● Margaret Anticline 	E-W regional shortening <ul style="list-style-type: none"> ● F₂ fold (Spartan Anticline) ● Strong penetrative N-S trending S₂ cleavage ● WNW-ESE sinistral strike-slip shearing along S₂ cleavage ● local shearing along S₂ (barren ore)
D ₃	NE-SW shortening <ul style="list-style-type: none"> ● Reactivation of all structures ● Dextral strike-slip faults and shear zones 	NW-SE to NNW-SSE compression and shearing <ul style="list-style-type: none"> ● steep and flat lying fractures (S₃) ● formation of WSZ, Watu shear ● sinistral reactivation of S₁ (SSZ) and S₂ ● local asymmetric fold (F₃) and crenulations ● NE-SW extensional veins & high grade Au in SSZ, CUS, and Margies etc. ● moderate grade mineralization ● felsic dykes intrusion
D ₄	NNW-SSE extension E-W lamprophyre dike intrusion	NW-SE shortening <ul style="list-style-type: none"> ● N-S fault development ● local dextral reactivation on S₃ surface ● high grade (1–2000 g/t) Au mineralisation in WSZ, WFZ, Summercloud, Predator lodes etc. ● steeply dipping (D_{4a}) and gently dipping (D_{4b}) vein ● relaxation and remobilization
Post-D ₄	-	NW-SE and NE-SW faults (D ₅ ?) EW shortening (D ₆ ?) <ul style="list-style-type: none"> ● sinistral, strike-slip subvertical faults EW extension <ul style="list-style-type: none"> ● intrusion of lamprophyre dykes

dextral normal offsets to the D_{4a} structures. A conjugate set of NW-SE and NE-SW faults (D₅?) postdate the ore and offset the stratigraphic package and ore zones. These are in turn offset by a set of sinistral, strike-slip subvertical faults with variable strikes (NNW-SSE to N-S, D₆?; Nugus and Biggam, 2007).

3.2. Mineralization Styles and Ore Assemblages

Mineralization styles vary in individual orebodies and also in different parts of the deposit depending on many factors, including, but not limited to, host lithology, configuration of the mineralizing trap, crosscutting relationships reflecting

a polyphase deformation history, and overlapping styles (Nugus *et al.*, 2005a).

The bulk of ore in all types of structures is contained within quartz-bearing veins that are mostly flat-dipping (Fig. 3A, B, and F), with characteristics such as vugs (Fig. 3A), pinch and swell geometries (Fig. 3B), and kinematic indicators that reflect an extensional regime. The nature and extent of brecciation are also important features in the deposit because brecciated veins and ore shoots account for most of the highest-grade ore. Breccia-hosted gold (Fig. 3C) mostly occurs in steeply-dipping orebodies, but can also occur in discrete zones along gently-dipping shear zones

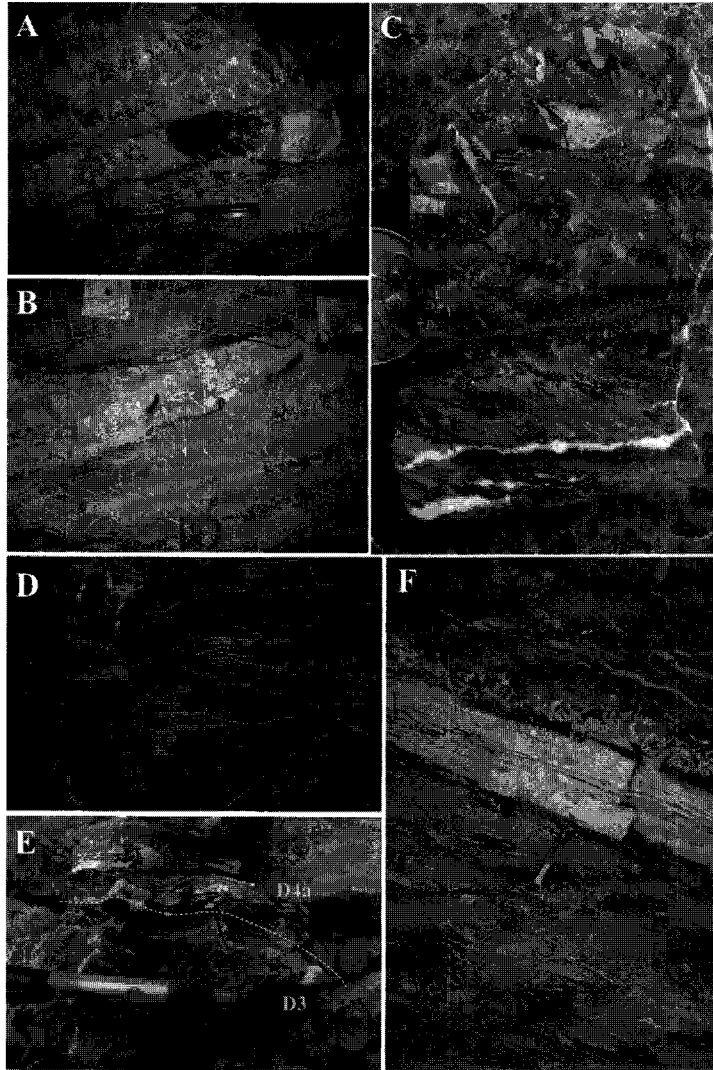


Fig. 3. Mineralization styles in the Sunrise Dam gold deposit. (A) A carbonate-sulfide filled vug in the D_{4b} stage auriferous vein. 2077 ore drive (OD), SSZ. (B) D_{4b} stage quartz vein showing pinch-and-swell structure. 2077 OD, SSZ. (C) Quartz carbonate breccia containing visible native gold. The ore grade is 1140 g/t Au. (D) Sulfidation of BIF along the fault plane (outlined by dotted lines), 2067 OD, SSZ. (E) D_{4a} vein crosscutting folded D_3 vein, WSZ open pit. Note more highly deformed and bleached appearance of D_3 veins. (F) Typical high grade D_{4b} vein showing stylolitic laminae. Note the intense brecciation and highly sheared fabric in the host rock. 2066 OD, SSZ.

(e.g., SSZ), which are enveloped by broader alteration halos than in the steeper counterparts. In some cases the precipitation of gold was caused, at least partly, by fluid-rock interaction that is marked by the sulfidation (replacement of magnetite by pyrite) of abundant BIF units (Fig. 3D).

The deposit is low in sulfides (<5 vol.%) because most of the economic ore occurs as coarse native gold within quartz. However, native gold is also

present as inclusions in some of the sulfides, especially in D_{4b} pyrites, as well as in Au-tellurides. Pyrite is the most common sulfide in the deposit and is present in variable amounts in ore-bearing zones and within alteration halos in the country rocks. Arsenopyrite is mostly known from the central, deeper part of the deposit (e.g., WSZ, WFZ, Astro, Cosmo, Dolly Volcanic, Dolly Porphyry, and GQ ore bodies; Fig. 2), but it also

occurs in the SSZ, especially where BIF units are present.

Typical D₃ quartz-carbonate veins are bleached in appearance, in some cases folded and display cusped-lobate interfaces with host rock (Fig. 3E). The ore minerals consist of minor amounts of arsenian pyrite and subordinate arsenopyrite. The D_{4a} veins are mainly composed of grayish white to dark gray quartz and ankerite, and show well-developed dark internal laminae (Fig. 3E and 5A). In contrast, the D_{4b} veins consist of vitreous to milky quartz (Fig. 3F) and more commonly display pinch-and-swell morphology (Fig. 3B) with thicknesses ranging from several cm to nearly 100 cm. Gangue minerals in D_{4b} veins are vitreous to milky quartz with minor amounts of ankerite, barite, rutile, chlorite, and muscovite. Coarse native gold, arsenopyrite, As-bearing pyrite and As-rich sulfosalts are mostly found in the D_{4a} veins, whereas D_{4b} veins are characterized by an increase in the abundance of base metals sulfides, Sb-rich sulfosalts, and tellurides. Compared with earlier veins, D₄ veins are characterized by the presence of minor amounts of telluride minerals. Stylolitic dark laminae, which are mainly composed of muscovite and tourmaline, have locally developed parallel to the veins (Fig. 3F).

Alteration assemblages comprising variable amounts of muscovite, chlorite, carbonates and fuchsite, are present in orebodies where BIF and/or (ultra)mafic rocks are encountered. Sericite is considered to track a proximal position to ore whereas chlorite is medial to distal. Carbonate minerals (dolomite, Fe-dolomite, ankerite) are more abundant in high-grade breccia bodies and veins enriched in base metals. Distinct Na-rich assemblages, formed by alteration of abundant albite, and which also include gold in pyrite, are described by Cleverley *et al.* (2006). One such assemblage consists of CO₂- and Sr-rich apatite with magnetite inclusions, rutile, dolomite ± zircon, within tourmaline-mica laminations from flat veins in SSZ. A second assemblage, observed within breccia from the underground GQ orebody comprises fuchsite-sulfide (As-bearing pyrite, molybdenite, fahlore) laminations in steeper veins.

The paragenesis of ore veins can be divided into five stages, which are broadly consistent with major deformation events (Fig. 4). The general

	D1	D2	D3	D4a	D4b
quartz					
albite					
K-feldspar					
muscovite (sericite)					
chlorite					
fuchsite					
magnetite					
scheelite					
chromite					
monazite					
cassiterite					
tourmaline					
fluorapatite					
rutile					
ankerite (dolomite)					
calcite					
strontianite					
celestine					
barite					
gypsum					
pyrite					
pyrrhotite					
arsenopyrite					
sphalerite					
chalcopyrite					
molybdenite					
galena					
stibnite					
tetrahedrite group					
gersdorffite					
bournonite					
zinkenite					
semseyite					
auristibite					
native gold (electrum)					
hessite					
altaite					
tetradymite					
melonite					
nagyagite					
petzite					
calaverite					
(Bi)-tellurantimony					
Au-(Ag)-As telluride					
Au-Sb-telluride					
Sb-tellurobismuthite					

Fig. 4. Paragenetic sequence of vein minerals in the Sunrise Dam deposit.

nature of stages is as follows:

- D₁: siliceous, fragmental veins with sulfide-poor matrix;
- D₂: quartz and carbonates (barren);
- D₃: quartz, carbonates, oxides, rare sulfides, and sulfosalts (moderate grade mineralization throughout the SSZ);
- D_{4a}: quartz, silicates, oxides, carbonates, sul-

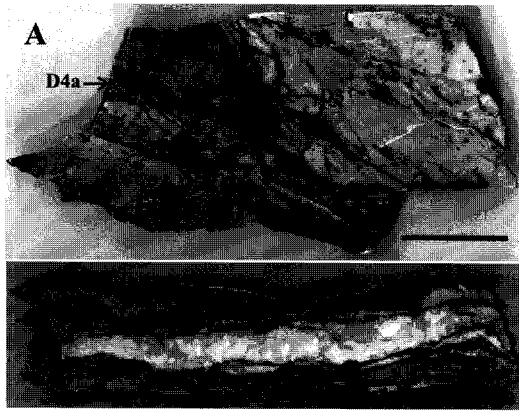


Fig. 5. Photographs illustrating textural relationships between D_3 and D_{4a} stages at Sunrise Dam. Scale bars are 5 cm. (A) D_{4a} dark gray ankerite-quartz vein crosscut D_3 veins mainly consisting of fine-grained pyrite (06-7, WSZ 2109 OD). (B) Typical D_{4a} vein consisting of gray quartz and pinkish white ankerite with stylolitic dark laminae along the vein salvage (06-21, SSZ open pit).

fides, sulfosalts, native gold, and tellurides (major mineralization);

- D_{4b} : quartz, silicates, oxides, phosphates, carbonates, sulfates, sulfides, sulfosalts, native gold (electrum), and tellurides (localized high grade).

Except for the D_{4a} and D_{4b} stages, all five stages are rarely observed at a single locality. One of the main reasons is that early-formed structures, such as D_1 , D_2 and D_3 were successively reactivated, truncated and overprinted by high-grade D_4 stage mineralization (Nugus and Biggam, 2007). Locally, however, some samples show more than one stage (Fig. 5A). In the D_{4b} stage, the more diverse association of telluride minerals can be attributed to post- D_{4b} mineralization (remobilization), which is commonly accompanied by small-scale reaction fronts and destabilization of earlier minerals at the scale of polished sections (Sung *et al.*, 2007).

Mineralization associated with D_1 and D_2 stages

The D_1 -stage mineralization was studied from sequences in the western wall of the Sunrise pit. This was sampled from a small remnant of quartz vein (dark gray) preserved within intensely folded D_3 veins, which are in turn crosscut by gently-dipping D_4 veins. The mineralization includes: fine-

grained pyrite (50~120 μm) as well as minor amounts of tennantite, chalcopyrite, and molybdenite. Tennantite is found as fine-grained disseminations in the host rock, and occasionally surrounded by other sulfides. Brown *et al.* (2002b) documented that quartz + chalcopyrite + molybdenite veins are spatially associated with rhyodacite porphyry dikes and are crosscut by Au-bearing Western Lodes. Based on mineralogical and structural interpretation (e.g., arsenopyrite-rich and steep-dipping), the Western Lodes corresponds to D_{4a} stage ore lodes (see below), and the quartz + chalcopyrite + molybdenite veins represent D_1 stage.

The D_2 stage is mostly represented by barren quartz \pm minor carbonate veins. Alteration assemblages attributed to the D_2 stage are consistent with those of regional metamorphism that are associated with the formation of the Spartan anticline. The bulk of ore deposition postdates the main deformation that resulted in the formation of the gently dipping shear zones (e.g., SSZ and CUS of D_1 deformation) and Spartan anticline (D_2 deformation).

Mineralization associated with the D_3 stage

The mineral associations attributed to the D_3 stage mainly include: quartz, ankerite and pyrite, with minor tennantite, chalcopyrite, pyrrhotite, magnetite, and rare scheelite. Nugus and Biggam (2007) also reported the occurrence of minor sericite, chlorite, albite, and arsenopyrite in the D_3 veins. The latter, however, has not been found in D_3 -stage samples studied here. Typical D_3 mineralization occurs as veins showing ductile deformation (e.g., folding and shearing; Fig. 5A). Massive pyrite, with coarse grains (up to cm-size), resulting from replacement of BIF units during the D_3 stage, is also observed in some orebodies.

Mineralization associated with the D_{4a} stage

D_{4a} stage is considered the main stage for gold deposition and it also has a diverse mineralogical character, resulting in the deposition of pyrite, arsenopyrite, and tennantite with minor to trace amounts of native gold, chalcopyrite, galena, gersdorffite, chromite, hessite, altaite, tetradymite, and melonite. Ore minerals account for approximately 5% of the total volume of vein filling. Although some of the sulfides/sulfosalts host some gold inclusions, visible gold is the main form of ore in

these veins. The vein-fill material is dark to pale gray quartz, pinkish white ankerite, and white dolomite. When veins are rich in arsenopyrite, they tend to appear darker (Fig. 5A) than sulfide-poor veins (Fig. 5B). The dark laminations in quartz-ankerite veins consist mainly of sheet silicate minerals, such as muscovite and chlorite with minor amounts of pyrite and quartz (Fig. 5B). Fuchsite is readily seen as an alteration mineral where BIF or (ultra)mafic rocks are encountered, especially in the central deeper part of the deposit (e.g., underground GQ ore body).

The main distinction between the D_3 and D_{4a} stages is the lack of pyrrhotite and abundance of arsenopyrite, arsenian pyrite, native gold and the occurrence of minor telluride minerals as inclusions in pyrite. Pyrite in the D_{4a} stage occurs as small subhedral to anhedral grains disseminated in the veins or in the altered host rocks (2–500 μm), coarser subhedral to euhedral grains showing zonal growth texture (up to 1 mm, Fig. 6A and B), and rare aggregates of polygonal pyrite grains (up to 5 mm). Some of the pyrites in the host rock are present as skeletal crystals enclosing anhedral chlorite cores. Zoning in D_{4a} pyrite is similar with that of D_3 stage pyrite. It consists of inclusion-rich low As core (zone I), narrow As-rich zone with arsenopyrite and/or native gold inclusions (zone II), and relatively inclusion-free overgrowth zone III (Fig. 6A). Native gold grains are infrequently found in the S-richer (As-poor) area of the 2nd zone and generally occur as tiny inclusions (<0.4 μm ; marked in circles in Fig 6A). Although this zoning is not visible on fresh polished surfaces, it

becomes evident after exposure to air for several weeks. The occurrence of visible gold in particular zone of arsenian pyrite is a common feature in some gold deposits from the EGP (Morey *et al.*, 2008), and Sung *et al.* (2009) recently described as a result of coupled dissolution-precipitation process, in which replacement occurs along a reaction front by full dissolution of the mineral followed by tightly coupled reprecipitation (Putnis, 2002). It appears that at Sunrise Dam such coupled dissolution-precipitation reactions may have been important in upgrading the ore grades during D_{4a} mineralization.

Arsenopyrite is the one of the dominant ore minerals in the D_{4a} stage, and its occurrences appear to be largely restricted in the central and deeper part of the deposit; e.g., WSZ, WFZ, Astro, Cosmo, Dolly Volcanic, Dolly Porphyry, and GQ ore bodies.

Mineralization associated with the D_{4b} stage

The D_{4b} mineralization is characterized by an increase in the abundance of base metal sulfides and Sb-dominant sulfosalts, and the occurrence of a variety of telluride species (Fig. 4). Ore minerals comprise only a small portion of the vein (usually <2%), mostly occurring as disseminations within quartz-ankerite veins and proximal alteration zones. Concentrations of ore minerals are rarely seen in this stage, but where present they consist of pyrite, sphalerite, galena, chalcopyrite, tetrahedrite-tennantite, with minor tellurides and gold, resulting in significant contribution to the total gold budget of the deposit.

The ore mineral association in D_{4b} stage includes

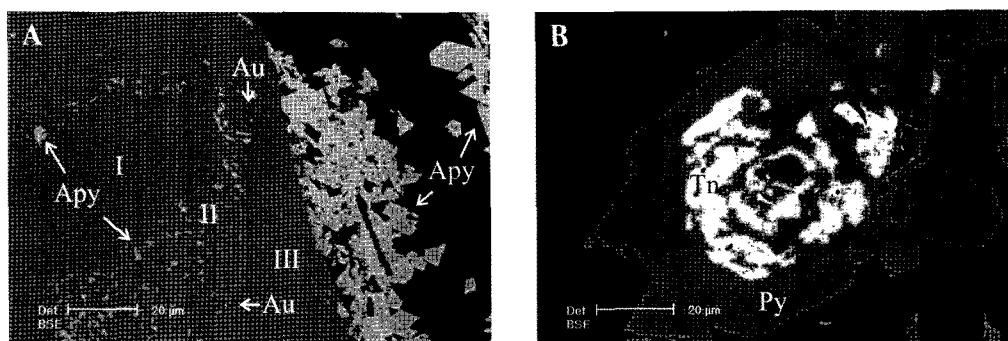


Fig. 6. SEM back-scattered images of D_{4a} pyrite mineralization. (A) Zoned pyrite overgrown by fine-grained arsenopyrite (Apy). Note extremely fine-grained (<400 nm) native gold grains (Au) of arsenopyrite-rich zone II (c-3, AST ugd728-54m). (B) Tennantite (Tn) inclusion in pyrite (4-5, CSM 1940 OD).

pyrite, sphalerite, tennantite-tetrahedrite, galena, chalcopyrite, molybdenite, stibnite, bournonite (PbCuSbS_3), zinkenite ($\text{Pb}_9\text{Sb}_{22}\text{S}_{42}$), gersdorffite (NiAsS), scheelite, cassiterite, native gold, electrum, aurostibite (AuSb_2), semseyite ($\text{Pb}_9\text{Sb}_8\text{S}_{21}$), and various tellurides [hessite (Ag_2Te), altaite (PbTe), tetradymite ($\text{Bi}_2\text{Te}_2\text{S}$), melonite (NiTe_2), nagyágite ($(\text{Pb,Sb})_6(\text{Au,Te})_3\text{S}_6$), petzite (Ag_3AuTe_2), calaverite (AuTe_2), tellurantimony (Sb_2Te_3), Bi-bearing tellurantimony ($(\text{Sb,Bi})_2\text{Te}_3$), Sb-bearing tellurobismuthite ($(\text{Bi,Sb})_2\text{Te}_3$), and two unnamed tellurides, (Au-Ag)-As telluride and Au-Sb-telluride]. Cleverly *et al.* (2006) reported small inclusions of kolarite (PbTeCl_2) within the tourmaline-mica laminations in the SSZ ore lodes. Pyrite is the most common sulfide mineral and also the major host for native gold inclusions in D_{4b} stage. The abundance of inclusions-rich and zoned-pyrite is less common

compared with the D_{4a} stage. Gangue minerals comprise quartz, ankerite, dolomite, muscovite, chlorite, fuchsite, tourmaline, fluorapatite, rutile, calcite, strontianite, celestine, barite, and gypsum.

Internal laminae, sometimes with stylolitic appearance are also found in the D_{4b} veins (Fig. 3F). In this case they consist of preferentially aligned muscovite - tourmaline - rutile - fluorapatite - pyrite \pm native gold and are thus more varied than the similar laminations present in the D_{4a} veins. Cleverly *et al.* (2006) reported small inclusions of kolarite (PbTeCl_2) within the tourmaline-mica laminations in the SSZ ore lodes.

3.3. Gold (Electrum) Mineralization

A large number of native gold grains were encountered in D_{4a} veins mostly occurring as micron-sized inclusions in sulfides (Fig. 6A, 7A

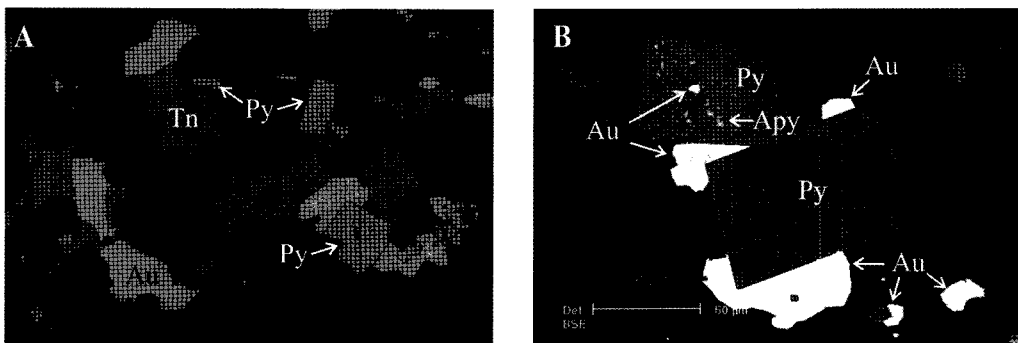


Fig. 7. Reflected light photomicrograph (A) and back-scattered electron images (B) of native gold in D_{4a} stage. (A) Native gold (Au) closely associated with tennantite (Tn) and pyrite (Py). Width of field is 2 mm (c-4, AST ugd728-55m). (B) Native gold occurring as overgrown grains on euhedral pyrite and as inclusion in As-rich area with arsenopyrite (Apy)(c-3, AST ugd728-54m).

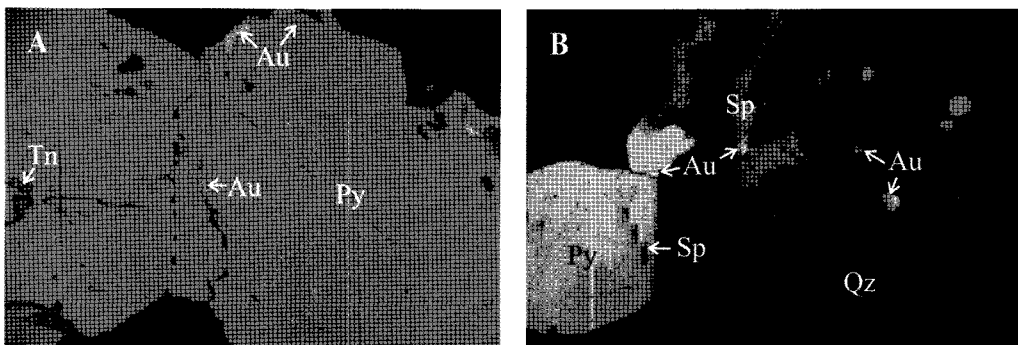


Fig. 8. Reflected light photomicrographs of native gold and electrum in D_{4b} stage. Width of field 2 mm. (A) Native gold (Au) and tennantite (Tn) inclusions along pyrite (Py) growth surfaces (su15-2, SSZ 2067 OD). (B) Gold grains occurring in sphalerite (Sp), in fractures of pyrite, and as free gold in quartz (Qz)(su15-2).

and B), as isolated grains in quartz-ankerite vein, as discrete rounded to ellipsoidal blebs overgrown on pyrite (Fig. 7B), coexisting with tennantite (Fig. 7A), and less commonly filling microfractures or grain boundaries in pyrite. Some larger gold grains have euhedral pyrite inclusions. Microscopic gold (<5–70 μm) is common, however, visible gold including spectacular showings of the noble metal, are encountered in certain parts of the mine (e.g., WSZ, WFZ, and Astro ore bodies).

In the D_{4a} stage ores, 52% of the microscopic gold (>2 μm in size, 111 grains in 50 polished blocks) is associated with other ore minerals and the remained (48%) are found as free gold. McQueen et al. (1994) studied the nature of pyritic gold ores in Golden Mile deposit, Kalgoorlie, Western Australia. They found that gold associated with pyrite occurs as both intragranular (within pyrite) and intergranular (between grain boundaries of pyrite) inclusions, with the ratio of 78% and 22% for each type. For the D_{4a} veins in the Sunrise Dam, the majority of gold grains (ca. 95%) are intragranular type within pyrite and only 5% occurs as intergranular type filling the fractures in pyrite.

Gold in the D_{4b} stage is always xenomorphic and appears in a variety of shapes from longer filaments to small “droplets”. Gold grains were found as free gold (<5–250 μm) in quartz-ankerite veins, tiny inclusions elongated along growth planes in pyrite (Fig. 8A), or filling microfractures, and at grain boundaries of pyrite (Fig. 8A and B). Gold inclusions in skeletal pyrite are most likely to be co-precipitated. Such textures have been interpreted as evidence for precipitation of gold transported as a bisulfide complex in the fluids (Proudlove and Hutchinson, 1989). Native gold also occurs as inclusions in minerals from the tetrahedrite-tennantite group, galena, sphalerite (Fig. 8B), and as a breakdown product of nagyágite (Sung et al., 2007).

The paragenetic location of native gold and electrum in the D_{4b} stage was also determined and counted for 401 grains in 13 polished blocks. According to this result, the best mineralogical indicator of gold content is pyrite (39%) followed by nagyágite (28%) and tennantite-tetrahedrite (13%). Only 12% of grains occur as free gold in quartz, the remainder is hosted in galena (5%),

hessite + altaite (3%), and the smallest proportion of grains is present within sphalerite (<1%). Although large numbers of gold grain were counted in nagyágite, they are associated with other breakdown minerals, such as semseyite, altaite, and aurostibite (Sung et al., 2007). Furthermore, nagyágite is found only in some swelling parts of gently dipping quartz veins from the underground SSZ ore body. Therefore, the best mineralogical indicator of gold content in both D_{4a} and D_{4b} stage should be ascribed to pyrite and the tetrahedrite-group minerals.

4. Conclusions

The paragenetic sequence of the Sunrise Dam deposit can be divided into five hydrothermal stages, which are supported by distinctive features of the mineralogical assemblages. Among them, the D_{4a} stage is the dominant episode of Au deposition, followed by the D_{4b} stage, which is characterized by more diverse ore mineralogy including base metal sulfides, sulfosalts, and telluride minerals. The D_{4a} stage contains higher proportions of microscopic free gold (48%) than D_{4b} stage (12%), and pyrite is the principal host for native gold (electrum) followed by tetrahedrite-group minerals in both stages. Coarse-grained pyrites commonly display three growth zones which may result from multiple fluid flow with different As/S ratios over a protracted period of time (from D_3 to post- D_{4a}). Among them, the second zone contains numerous inclusions of arsenopyrite with high concentration of Au (Sung et al., 2009), which is interpreted as a product of coupled dissolution-reprecipitation process (Putnis, 2002) responsible for upgrading Au grade in D_{4a} mineralization.

Acknowledgments

We wish to thank for Korea Resources Corporation (KORES), Anglo-Gold Ashanti Australia, and the South Australian Museum for financial support for the research project.

References

- Barley, M.E., Brown, S.J.A., Krapez, B. and Cas, R.A.F. (2002) Tectonostratigraphic analysis of the Eastern Yilgarn Craton: An improved geological framework for

- exploration in Archaean terranes. Perth, Amira International Limited.
- Barley, M.E., Eisenlohr, B.N., Groves, D.I., Perring, C.S. and Vearncombe, J.R. (1989) Late Archaean convergent margin tectonics and gold mineralization: A new look at the Norseman-Wiluna Belt. *Geology*, v.17, p.826-829.
- Blewett, R.S., Champion, D.C., Whitaker, A.J., Bell, B., Nicoll, M., Goleby, B.R., Cassidy, K.F. and Groenewald, P.B. (2002) Three dimensional model of the Leonora-Laverton transect area: implications for Eastern Goldfields tectonics and mineralisation. *GA-GSWA NorthEastern Yilgarn Workshop*. Perth, Western Australia, Geoscience Australia.
- Brown, S.M., Fletcher, I.R., Stein, H.J., Snee, L.W. and Groves, D.I. (2002a) Geochronological constraints on pre-, syn-, and postmineralization events at the world-class Cleo gold deposits, Eastern Goldfields Province, Western Australia. *Economic Geology*, v.97, p.541-559.
- Brown, S.M., Groves, D.I. and Newton, P.J.N. (2002b) Geological setting and mineralization model for the Cleo gold deposit, Eastern Goldfields Province, Western Australia. *Mineralium Deposita*, v.37, p.704-721.
- Brown, S.M., Johnson, C.A., Watling, R.J. and Premo, W.R. (2003) Constraints on the composition of ore fluids and implications for mineralising events at the Cleo gold deposit, Eastern Goldfields Province, Western Australia. *Australian Journal of Earth Science*, v.50, p.19-38.
- Cassidy, K.F., Champion, D.C., Krapez, B., Barley, M.E., Brown, S.J.A., Blewett, R.S., Groenewald, P.B. and Tyle, I.M. (2006) A revised geological framework for the Yilgarn Craton, Western Australia. Western Australia Geological Survey.
- Cassidy, K.F. and Hagemann, S.G. (2001) World-class Archaean orogenic gold deposits, eastern Yilgarn Craton: Diversity in timing, structural controls and mineralization styles. *Geoscience Australia*, p.382-384.
- Cleverley, J.S., Nugus, M. and Young, C. (2006) Gold in Na-assemblages: Implications for deep fluid sources and pathways in the Eastern Goldfields. *predictive mineral discovery CRC conference*. Perth, Western Australia.
- Griffin, T.J. (1990) Eastern Goldfields Province. In Playford, P.E. (Ed.) *Geology and Mineral Resources of Western Australia*. Perth, Geological Survey of Western Australia.
- Hallberg, J.A. (1985) *Geology and mineral deposits of Leonora-Laverton Area, northeastern Yilgarn Block, Western Australia*, Hesperian Press, Victoria Park, Western Australia.
- Krapez, B., Brown, S.J., Hand, J., Barley, M.E. and Cas, R.A. (2000) Age constraints on recycled crustal and supracrustal sources of Archaean metasedimentary sequences, Eastern Goldfields Province, Western Australia; evidence from SHRIMP zircon dating. *Tectonophysics*, v.322, p.89-133.
- McQueen, K.G., Bielin, S. and Lennie, C.A. (1994) *The nature of pyritic gold ores at Kalgoorlie, Western Australia: Geological and metallurgical implications*, Economic Geology Research Unit, James Cook University of North Queensland.
- Morey, A.A., Tomkins, A.G., Bierlein, F.P., Weinberg, R.F. and Davidson, G.J. (2008) Bimodal distribution of gold in pyrite and arsenopyrite: examples from the Archaean Boorara and Bardoc shear systems, Yilgarn Craton, Western Australia. *Economic Geology*, v.103, p.599-614.
- Myers, J.S. (1997) Preface: Archaean geology of the Eastern Goldfields of Western Australia-regional overview. *Precambrian Research*, v.83, p.1-10.
- Myers, J.S. and Hickman, A.H. (1990) Pilbara and Yilgarn Cratons-regional geology and mineralizations. In Hughes, F.E. (Ed.) *Geology of the Mineral Deposits of Australia and Papua New Guinea*. The Australasian Institute of Mining and Metallurgy.
- Newton, P.G.N., Tornatora, P.M.A., Smith, R. and Clifford, M. (2002) The Cleo-Sunrise Au deposit, Laverton, WA: contrasting structural styles within a thrust duplex. *Applied Structural Geology for Mineral Exploration and Mining*. Kalgoorlie.
- Newton, P.J.N., Gibbs, D., Grove, A., Jones, C.M. and Ryall, A.W. (1998) Sunrise-Cleo gold deposit. In Berkman, D.A. and Mackenzie, D.H. (Eds.) *Geology of Australian and Papua New Guinean mineral deposits*. The Australasian Institute of Mining and Metallurgy.
- Nugus, M. and Biggam, J. (2007) Geology of Sunrise Dam Gold mine. Internal technical report. AngloGold Ashanti Australia.
- Nugus, M., Biggam, J. and Blenkinsop, T. (2005a) Controls and distribution of gold mineralisation within Sunrise Shear Zone-implications for resource estimation and mining. *Best Practice and Innovation in Global Mine Geology, 29 May - 3 June*. Economic Geology Research Unit, School of Earth Sciences, James Cook University, Publication 64: 99.
- Nugus, M., Blenkinsop, T., Biggam, J. and Doyle, M. (2005b) The role of early-formed structure in lode gold mineralisation: The Sunrise Dam gold Mine, Yilgarn Craton, WA. *Best Practice and Innovation in Global Mine Geology, 29 May - 3 June*. Economic Geology Research Unit, School of Earth Sciences, James Cook University, Publication 64: 99.
- Nugus, M., Blenkinsop, T., Mcleod, T., Doyle, M. and Kent, M. (2005c) Structural control of gold mineralisation by reactivation of backthrusts at Sunrise Dam Gold Mine, Yilgarn Craton, WA. *Best Practice and Innovation in Global Mine Geology, 29 May - 3 June*. Economic Geology Research Unit, School of Earth Sciences, James Cook University, Publication 64: 99.
- Nugus, M.J., Blenkinsop, T.G. and Mclellan, J.G. (2006) Creation of a world-class deposit Archaean lode gold deposit through multiple reactivations of geological structures. *Australian Earth Sciences Convention, Melbourne, 2-6th July, GSA Conference Abstract series: 168*. Melbourne.
- Ojala, V.J. (1995) Structural and depositional controls on gold mineralization at the Granny Smith Mine, Laverton, Western Australia. University of Western Australia.
- Ojala, V.J., Ridley, J.R., Groves, D.I. and Hall, G.C. (1993) The Granny Smith gold deposit: The role of heterogeneous stress distribution at an irregular granitoid contact in a greenschist facies terrane. *Mineralium Deposita*, v.28, p.409-419.
- Proudlove, D.C. and Hutchinson, R.W. (1989) Multiphase mineralization in concordant and discordant gold veins,

- Dome Mine, South Porcupine, Ontario, Canada. In Keays, R. and Skinner, B. J. (Eds.) *Economic Geology Monograph*.
- Putnis, A. (2002) Mineral replacement reactions: From macroscopic observations to microscopic mechanisms. *Mineralogical Magazine*, v.66, p.689-708.
- Salier, B.P., Groves, D.I., Menaughton, N.J. and Fletcher, I.R. (2005) Geochronological and stable isotope evidence for widespread gold mineralization from a deep-seated fluid source at ca. 2.65 Ga in the Laverton Gold Province, Western Australia. *Economic Geology*, v.100, p.1363-1388.
- Sung, Y.-H., Ciobanu, C.L., Pring, A., Brugger, J., Skinner, W., Cook, N.J. and Nugus, M. (2007) Tellurides from Sunrise Dam gold deposit, Yilgarn Craton, Western Australia: a new occurrence of nagyágite. *Mineralogy and Petrology*, v.91, p.249-270.
- Sung, Y.-H., Ciobanu, C.L., Pring, A., Brugger, J., Skinner, W. and Nugus, M. (2009) Invisible gold in arsenian pyrite and arsenopyrite from a multistage Archean gold deposit: Sunrise Dam, Eastern Goldfields Province, Western Australia. *Mineralium Deposita*, v.44, p.765-791.
- Swager, C.P. (1997) Tectono-stratigraphy of late Archean greenstone terranes in the southern Eastern Goldfields, Western Australia. *Precambrian Research*, v.83, p.11-42.

2010년 10월 1일 원고접수, 2010년 10월 20일 게재승인